the plant journal

SEB Society for Experimental Biology

The Plant Journal (2015) **84,** 360–373 doi: 10.1111/tpj.13004

Light acclimation involves dynamic re-organization of the pigment–protein megacomplexes in non-appressed thylakoid domains

Marjaana Suorsa[1], Marjaana Rantala[1], Fikret Mamedov[2], Maija Lespinasse[1], Andrea Trotta[1], Michele Grieco[1,†], Eerika Vuorio[1], Mikko Tikkanen[1], Sari Järvi[1] and Eva-Mari Aro[1,*]

[1]Department of Biochemistry, Molecular Plant Biology, University of Turku, FI-20014 Turku, Finland, and

[2]Molecular Biomimetics, Department of Chemistry – Ångström Laboratory, Uppsala University, Box 523, 75120 Uppsala, Sweden

Received 21 December 2014; revised 20 August 2015; accepted 24 August 2015; published online 29 August 2015.

*For correspondence (e-mail evaaro@utu.fi).

†Present address: Department of Ecogenomics and Systems Biology, University of Vienna, Althanstrasse 14, A-1090, Vienna, Austria.

The copyright line for this article was changed on 27 November 2015 after original online publication.

SUMMARY

Thylakoid energy metabolism is crucial for plant growth, development and acclimation. Non-appressed thylakoids harbor several high molecular mass pigment–protein megacomplexes that have flexible compositions depending upon the environmental cues. This composition is important for dynamic energy balancing in photosystems (PS) I and II. We analysed the megacomplexes of Arabidopsis wild type (WT) plants and of several thylakoid regulatory mutants. The *stn7* mutant, which is defective in phosphorylation of the light-harvesting complex (LHC) II, possessed a megacomplex composition that was strikingly different from that of the WT. Of the nine megacomplexes in total for the non-appressed thylakoids, the largest megacomplex in particular was less abundant in the *stn7* mutant under standard growth conditions. This megacomplex contains both PSI and PSII and was recently shown to allow energy spillover between PSII and PSI (*Nat. Commun.*, 6, 2015, 6675). The dynamics of the megacomplex composition was addressed by exposing plants to different light conditions prior to thylakoid isolation. The megacomplex pattern in the WT was highly dynamic. Under darkness or far red light it showed low levels of LHCII phosphorylation and resembled the *stn7* pattern; under low light, which triggers LHCII phosphorylation, it resembled that of the *tap38/pph1* phosphatase mutant. In contrast, solubilization of the entire thylakoid network with dodecyl maltoside, which efficiently solubilizes pigment–protein complexes from all thylakoid compartments, revealed that the pigment–protein composition remained stable despite the changing light conditions or mutations that affected LHCII (de)phosphorylation. We conclude that the composition of pigment–protein megacomplexes specifically in non-appressed thylakoids undergoes redox-dependent changes, thus facilitating maintenance of the excitation balance between the two photosystems upon changes in light conditions.

Keywords: *Arabidopsis thaliana*, light acclimation, native gel electrophoresis, non-appressed thylakoid, phosphorylation, protein complex.

INTRODUCTION

The chloroplast thylakoid membrane hosts the major photosynthetic protein complexes photosystems (PS) II and PSI together with their light-harvesting complexes (LHC)II and LHCI, the cytochrome (Cyt) b_6f complex and ATP synthase. High protein density, particularly in grana appressions, ensures efficient light absorption and energy transfer (Kirchhoff *et al.*, 2002, 2004) between the densely packed PSII–LHCII supercomplex macrodomains. PSI, ATP synthase and the chloroplast NAD(P)H dehydrogenase (NDH)-like complex, conversely, are enriched in non-appressed thylakoid domains (Dekker and Boekema, 2005; Kirchhoff, 2013; Pribil *et al.*, 2014; Suorsa *et al.*, 2014).

For a long time, the PSII–LHCII supercomplexes in the appressed grana thylakoid domains have been the most extensively – and practically exclusively – studied large protein complexes in the higher plant thylakoid membrane. Recent progress in electron microscopy and atomic force microscopy has enabled the formation of a rather

detailed picture of the supramolecular organization of the PSII–LHCII super- and megacomplexes in grana thylakoids (Dekker and Boekema, 2005; Caffarri *et al.*, 2009; Herbstova *et al.*, 2012; Kouril *et al.*, 2013; Tietz *et al.*, 2015). Two other high molecular mass thylakoid protein complexes, PSI–LHCI–LHCII (Pesaresi *et al.*, 2009) and PSI–NDH (Peng *et al.*, 2008), have likewise been well characterized. The latter functions in NDH-like dependent cyclic electron transfer (CET), whereas the PSI–LHCI–LHCII supercomplex has a role in distribution of excitation energy between the two photosystems. In wild type (WT) plants, phosphorylation of LHCII, catalysed by STN7 kinase, enhances the formation of this particular complex and, conversely, dephosphorylation of LHCII by TAP38/PPH1 (hereafter TAP38) phosphatase disassembles the complex. This mechanism has been shown to bear a fundamental role in dynamic light acclimation (Tikkanen *et al.*, 2006; Brautigam *et al.*, 2009; Pesaresi *et al.*, 2009; Pribil *et al.*, 2010; Shapiguzov *et al.*, 2010; Wientjes *et al.*, 2013a).

Recently, a large pore blue native (lpBN) gel electrophoresis method, originally developed for the separation of high molecular mass mitochondrial megacomplexes (Strecker *et al.*, 2010), was optimized for analyses of the thylakoid membrane megacomplexes (Jarvi *et al.*, 2011). Additionally, it was demonstrated that the mild non-ionic detergent digitonin is particularly suitable for characterization of megacomplexes in non-appressed thylakoid regions, due to its capacity to maintain weak protein–protein interactions (Jarvi *et al.*, 2011). Intriguingly, by application of mild digitonin solubilization and subsequent lpBN gel electrophoresis analysis, it was demonstrated that PSII and PSI form functional megacomplexes in non-appressed thylakoid membranes (Yokono *et al.*, 2015). The technical progress in gel-based analyses of thylakoid membrane megacomplexes, together with the above-mentioned and other recent reports on dynamics of the thylakoid protein complexes (Dietzel *et al.*, 2011; Galka *et al.*, 2012; Wientjes *et al.*, 2013b; Iwai *et al.*, 2014; Grieco *et al.*, 2015), prompted us to perform detailed analyses on membrane complexes residing in non-appressed thylakoid domains (Kettunen *et al.*, 1995), known to be highly dynamic upon light acclimation (Albertsson, 2001; Anderson *et al.*, 2012; Kirchhoff, 2013). To this end, a two-dimensional (2D) 'map' of the digitonin-solubilized thylakoid membrane proteins and protein complexes/megacomplexes in non-appressed thylakoid domains was first constructed from the WT. Subsequently, both short- and long-term acclimation responses of non-appressed thylakoid membrane protein complexes were analysed in parallel from both WT and several *Arabidopsis* mutant lines that were defective in photosynthesis acclimation regulatory proteins. We show that the composition of pigment–protein megacomplexes specifically in the non-appressed thylakoids undergoes redox-dependent changes, thus facilitating the maintenance of an excitation balance between the two photosystems upon changes in light conditions.

RESULTS

Proteomic analysis of non-appressed thylakoid membranes

A proteome view of non-appressed thylakoid domains (i.e. the other thylakoid domains except the tight grana core appressions) was first constructed from WT Arabidopsis plants grown under moderate light (120 μmol photons m^{-2} sec^{-1}, 8 h photoperiod). Thylakoids were isolated from 5-week-old plants 2 h after the onset of illumination and subjected to solubilization with digitonin. It is known that digitonin preferentially solubilizes the stroma-exposed thylakoid regions, whereas the inner parts of the grana stacks, highly enriched in PSII, remain largely unsolubilized (Jarvi *et al.*, 2011). This effect was reflected in a higher chlorophyll (Chl) *a*/*b* ratio of digitonin-solubilized thylakoid fraction, 4.08 ± 0.32 [mean ± standard deviation (SD), $n = 9$], compared with the Chl *a*/*b* ratio of 3.3 of intact thylakoids. Noteworthy, the Chl *a*/*b* ratio of the digitonin-solubilized membrane fraction was not as high as that typically obtained for highly purified stroma thylakoid fractions (Suorsa *et al.*, 2014). This result indicates that the digitonin treatment applied here prior to lpBN-PAGE also releases the protein complexes from the interphases (grana margins) between the grana thylakoids and genuine stroma-exposed thylakoids. This thylakoid fraction is known to contain relatively high concentrations of not only PSII and LHCII, but also PSI (Albertsson, 2001; Danielsson and Albertsson, 2009). Solubilized thylakoid fractions were subjected to 2D lpBN/SDS-PAGE, the gels were silver stained and protein spots were identified by mass spectrometry (Figure 1 and Table 1).

Besides the structural subunits of the major thylakoid membrane protein complexes, several regulatory proteins were also identified and localized to distinct complexes. For instance, the non-photochemical quenching (NPQ) trigger protein PsbS was found to be present as a diffuse spot in digitonin-solubilized thylakoid membranes, migrating both with megacomplexes (spot number 18) and with a lower molecular mass complex (spot number 19). Furthermore, a complex containing two recently characterized CURVATURE THYLAKOID1 proteins CURT1B and CURT1A (Armbruster *et al.*, 2013) was identified. Of the lumenal proteins, TLP18.3, which participates in PSII repair cycle (Sirpio *et al.*, 2007), was found to co-migrate with the PSII monomers (Figure 1). The non-appressed thylakoids were found to also host several other regulatory proteins, such as ALLENE OXIDE SYNTHASE (AOS, CYP74A), which has been shown to function in jasmonic acid biosynthetic pathway (Laudert *et al.*, 1996; Kubigsteltig *et al.*, 1999), CAS

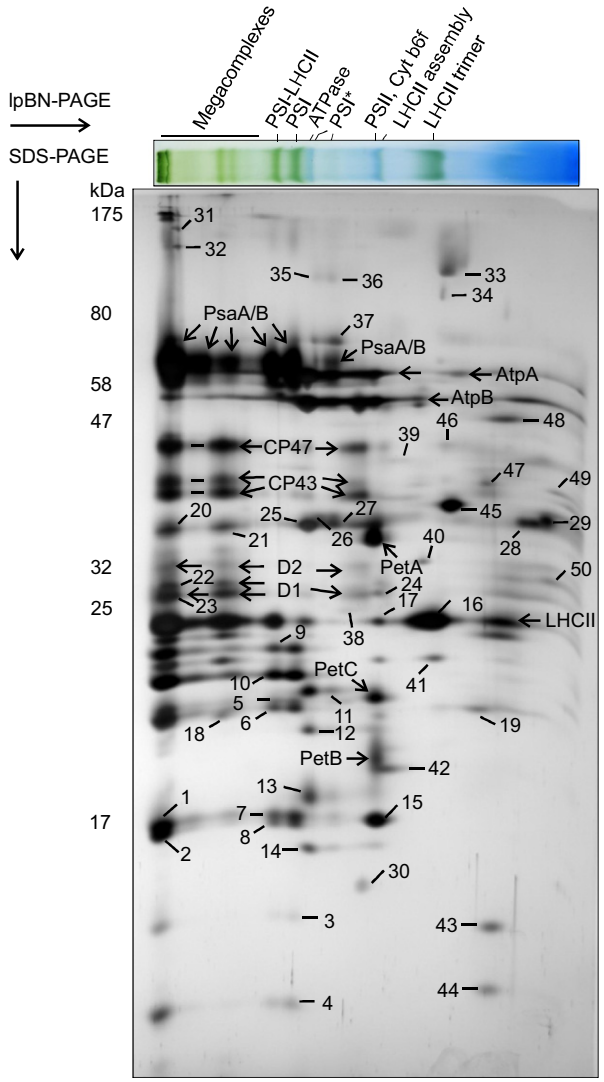

Figure 1. Proteomic analyses of non-appressed thylakoid domains.
Thylakoids were isolated from wild type (WT) Arabidopsis leaves acclimated to moderate growth light. Thylakoids were solubilized with digitonin and the protein complexes were separated with lpBN-PAGE. After electrophoresis, an lpBN lane was cut out, solubilized with Laemmli buffer and subjected to SDS-PAGE to detect the individual components of protein complexes. After staining the gel with silver, the individual proteins were cut out, digested with trypsin and identified by mass spectrometry. The proteins identified in this study are marked as numbers and listed in Table 1, whereas those identified based on Jarvi *et al.* (2011) are marked with their names.

(Vainonen *et al.*, 2008) and FLZ, which is a FZO-like protein and regulates thylakoid structure (Gao *et al.*, 2006). Intriguingly, besides PSI–LHCI, the PSI core proteins Psa*A*/*B* were also present in two smaller complexes that were devoid of LHCI but co-migrated with FTSH proteases (Wagner *et al.*, 2012), ferredoxin-NAPD$^+$-oxidoreductase (FNR) and TRANSLOCON AT THE INNER ENVELOPE MEMBRANE OF CHLOROPLASTS 62 (TIC62), which has been shown to form a complex with FNR (Benz *et al.*, 2009). In addition, thylakoid proteins with yet-unidentified functions – the proline-rich family protein AT5G07020 and the lumenal THYLAKOID LUMEN PEPTIDYL-PROLYL CIS-TRANS ISOMERASE OF 38 kDa (TLP38, also named as CYP37) – were likewise identified.

Megacomplexes of the non-appressed thylakoid membrane domains

To get an insight into the relationship between thylakoid regulation systems and thylakoid megacomplex formation/dynamics, the patterns of protein complexes from Arabidopsis WT and several mutant lines that were deficient in (de)phosphorylation of LHCII or PSII core proteins and/or regulation of NPQ, were analysed. The megacomplex composition of non-appressed thylakoid regions of the LHCII phosphorylation-deficient *stn7* mutants (*stn7* and *npq4 stn7*) differed from that of WT (Figure 2a, left panel). In line with this finding, the LHCII phosphatase overexpression mutant *oetap38*, which has only marginal capacity to keep LHCII phosphorylated and therefore shares several characteristics with *stn7* (Pribil *et al.*, 2010), showed a megacomplex composition similar to that of *stn7* (Figure S1b). In contrast, the *tap38*/*pph1* mutant (hereafter *tap38*), which lacks LHCII protein dephosphorylation, did not show any difference in the protein megacomplex composition as compared with WT. Furthermore, the *stn8* and *pbcb* mutants, which were incapable of phosphorylating and dephosphorylating the PSII core proteins respectively, possessed a megacomplex composition similar to that of the WT (Figure 2a, left panel). Likewise, the *npq4* and *oepsbs* mutants, demonstrating a lack or increased amount, respectively, of the NPQ-trigger protein PsbS, exhibited a WT-like megacomplex composition. The WT-like pattern of the non-appressed thylakoid megacomplex composition was also typical for the *ndho* and *ndh45* mutants, which were deficient in the thylakoid NDH-like complex (Sirpio *et al.*, 2009), as well as for the *pgr5* mutant, which was incapable of forming a proper transthylakoid proton gradient (Munekage *et al.*, 2002) (Figure S1a).

To dissect whether the distinctive *stn7* megacomplex composition is a direct consequence of the lack of LHCII protein phosphorylation or whether it possibly results from indirect long-term acclimation responses (previously shown to be triggered by the mutation) (Pesaresi *et al.*, 2009), WT plants were exposed for short time periods to different light qualities in order to manipulate LHCII phosphorylation prior to thylakoid isolation. A 1-h treatment with far red light ('state 1 light') not only induced disappearance of the classical state transition complex composed of PSI, LHCI and LHCII (Pesaresi *et al.*, 2009) but, importantly, also changed the entire megacomplex composition to resemble that of the *stn7* mutant (Figure 2a, right panel). Treatment with red light ('state 2 light'), in turn, resulted in a protein complex pattern that resembled that

Table 1 Proteins identified from non-appressed thylakoids with two-dimensional lpBN/SDS-PAGE

Spot no	Protein name (alternative names)	AGI code	MW (kDa) total predicted/-TP[a]	Peptides matched/ total	Cover (%)	Score
1	PsaF	AT1G31330	24.2/20.7	10/49	38	649
2	PsaE2	AT2G20260	15.2/10.6	9/9	46	212
	PsaE1	AT4G28750	15.0/10.5	8/9	54	229
3	PsaH	AT1G52230	15.3/10.8	4/4	19	100
4	PsaG	AT1G55670	17.1/11.1	6/22	21	263
5	PsaD2	AT1G03130	22.3/17.7	1/9	49	704
	PsaD1	AT4G02770	22.6/17.9	1/9	50	637
6	PsaD2	AT1G03130	22.3/17.7	1/10	52	672
	PsaD1	AT4G02770	22.6/17.9	1/10	50	641
7	PsaF	AT1G31330	24.2/20.7	9/12	44	565
8	PsaE1	AT4G28750	15.0/10.5	4/6	57	304
	PsaL	AT4G12800	23.1/18.0	4/6	26	403
9	Lhca1	AT3G54890	26.0/23	3/6	15	336
10	Lhca3	AT1G61520	29.2/23.7	7/10	22	268
11	AtpD	AT4G09650	25.7/20.5	6/10	31	576
12	AtpB	AT4G32260	23.9/16.2	12/21	37	510
13	AtpF	ATCG00130	21.1	12/37	35	748
14	AtpE	ATCG00470	14.5	8/31	56	370
15	PetD	ATCG00730	17.4	5/15	18	172
16	Lhcb1[b]	[b]		4/17	11	364
17	Lhcb1[b]	[b]		2/8	40	431
18	Lhcb6 (CP24)	AT1G15820	27.5/22.3	7/12	33	643
	PsbS	AT1G44575	28.0/21.6	6/9	37	475
19	PsbS	AT1G44575	28.0/21.6	6/8	18	116
20	PsbO1	AT5G66570	35.1/32.1/26.6[c]	4/26	63	1368
	PsbO2	AT3G50820	35.0/32.1/26.6[c]	4/23	67	1202
21	PsbO1	AT5G66570	35.1/32.1/26.6[c]	3/23	61	1131
	PsbO2	AT3G50820	35.0/32.1/26.6[c]	3/21	59	1110
22	D1	ATCG00020	32	10/10	28	595
	Lhcb4.1 (CP29.1)	AT5G01530	31.1/27.2	4/9	26	456
	Lhcb4.2 (CP29.2)	AT3G08940	31.1/27.2	11/16	42	839
23	D1	ATCG00020	32	10/10	28	618
	Lhcb4.1 (CP29.1)	AT5G01530	31.1/27.2	7/15	43	760
	Lhcb4.2 (CP29.2)	AT3G08940	31.1/27.2	6/14	44	570
24	D1	ATCG00020	32	8/9	23	546
	Lhcb4.1 (CP29.1)	AT5G01530	31.1/27.2	3/7	25	421
	LIGHT-HARVESTING-LIKE PROTEIN 3.1 (Lil3.1)	AT4G17600	29.4/25.1	5/6	20	353
	Lhcb4.2 (CP29.2)	AT3G08940	31.1/27.2	2/5	18	266
25	FERREDOXIN-NADP OXIDOREDUCTASE1 (FNR1)	AT5G66190	40.3/33.6	14/23	57.5	1054
	AtpC (ATP γ subunit)	AT4G04640	40.9/36.5	9/11	39.4	528
	CALCIUM SENSING RECEPTOR (CAS)	AT5G23060	41.3/37.8	10/11	32.3	514
26	FERREDOXIN-NADP OXIDOREDUCTASE1 (FNR1)	AT5G66190	40.3/33.6	20/27	62	1494
27	FERREDOXIN-NADP OXIDOREDUCTASE1 (FNR1)	AT5G66190	40.3/33.6	19/27	58	1370
28	FERREDOXIN-NADP OXIDOREDUCTASE2 (FNR2)	AT1G20020	41.2/35.2	17/33	29	354
29	FERREDOXIN-NADP OXIDOREDUCTASE1 (FNR1)	AT5G66190	40.3/33.6	30/81	55	1053
30	RbcS	AT5G38430	20.3/14.9	8/18	34	236
31	2-OXOGLUTARATE DEHYDROGENASE, E1	AT3G55410	115.2/115.2	9/9	9	435
32	LIPOXYGENASE2 (LOX2)	AT3G45140	102.1/95.8	15/15	17	801
33	ALPHA-GLUCAN PHOSPHORYLASE H (PHS2)	AT3G46970	95.2	25/32	46.14	1405
	FZO-LIKE PROTEIN	AT1G03160	100.7/94.6	16/18	22.04	764

(continued)

Table 1. (continued)

Spot no	Protein name (alternative names)	AGI code	MW (kDa) total predicted/-TP[a]	Peptides matched/ total	Cover (%)	Score
	GLYCINE DEHYDROGENASE (GLDP1)	AT4G33010	112.9	13/33	35.68	1491
	LIPOXYGENASE2 (LOX2)	AT3G45140	102.1/95.8	18/18	20.2	741
34	ALPHA-GLUCAN PHOSPHORYLASE H (PHS2)	AT3G46970	95.2	44/60	48	1192
35	TIC62	AT3G18890	68.3/61.24 Experimental: >100[d]	16/24	37	1206
36	TIC62	AT3G18890	68.3/61.24 Experimental: >100[d]	10/12	20	710
37	FTSH2	AT2G30950	74.2/69.2	17/39	54	2020
	FTSH8	AT1G06430	73.2/69.3	8/8	45	1531
38	THYLAKOID LUMEN PROTEIN 18.3 (TLP18.3)	AT1G54780	31.1/22.6/22.2 Experimental: >25[e]	12/13	45.26	652.51
39	FORMATE DEHYDROGENASE (FDH)	AT5G14780	42.4	19/23	67.24	894.14
40	NAD-MALATE DEHYDROGENASE2 (PMDH2)	AT5G09660	37.4	13/17	54.65	931.75
41	CARBONIC ANHYDRASE (CA1)	AT3G01500	29.5 Experimental: 21.3[f]	8/9	35.91	427.91
42	RIBOSOMAL PROTEIN L12, cp	AT3G27830	20.1/13.9	9/11	36	224
	THYLAKOID LUMENAL 15 kDa PROTEIN	AT2G44920	22.43/18.72/13.68[c]	4/4	20	190
	PetB	ATCG00720	24.1	4/4	19	158
43	CURVATURE THYLAKOID 1B (CURT1B)	AT2G46820	18.5/13.9	6/10	35	176
44	CURVATURE THYLAKOID 1A (CURT1A)	AT4G01150	17.7/11.2	7/10	24	157
45	FRUCTOSE-BISPHOSPHATE ALDOLASE 2	AT4G38970	43.0/38.0	17/26	34	684
46	SUCCINYL-COA-LIGASE8	AT2G20420	45.3/45.3	22/24	40	444
47	CYSTEINE SYNTHASE C1 (CYSC1)	AT3G61440	39.9	11/13	27	342
48	ALLENE OXIDE SYNTHASE (AOS, CYP74A)	AT5G42650	58.2/54.8	32/38	65.25	1608.16
49	THYLAKOID LUMEN PPIASE OF 38 kDa (TLP38)	AT3G15520	50.5/43.1/37.8[c]	17/23	26	449
50	Proline-rich family protein	AT5G07020	24.4	4/9	14	152
	Unknown protein	AT5G37360	33.4/27.6	4/4	13	116

TP, transit peptide.
Mass spectrometry analyses were performed from protein spots indicated in Figure 1.
[a]For nuclear-encoded chloroplast proteins [obtained from The Arabidopsis Information Resource (TAIR), www.arabidopsis.org, and from The Plant Proteome Database, http://ppdb.tc.cornell.edu/].
[b]The amino acid sequence cannot be used to distinguish between the five gene products of Lhcb1.
[c]Without the lumenal transit peptide.
[d]Lintala *et al.* (2014).
[e]In SDS-PAGE containing 6M urea (Sirpio *et al.*, 2007).
[f]Peltier *et al.* (2002).

of the non-appressed thylakoid regions isolated from WT leaves exposed to growth light.

Coomassie blue staining of the lpBN strip of the WT or *stn7* thylakoids (Figure 2b) revealed in total nine megacomplexes (i.e. complexes with a higher molecular mass than that of the classical state transition complex) in non-appressed thylakoids (Figure 2b and Table 2). The composition of each photosynthetic megacomplex was analysed by two-dimensional (2D) lpBN/SDS-PAGE (Figure 2c). As the nomenclature of the thylakoid membrane megacomplexes has not yet become established, and previous analyses of megacomplexes were based merely on WT thylakoids (Jarvi *et al.*, 2011; Wientjes *et al.*, 2013a), a more comprehensive nomenclature for the megacomplexes is introduced here (Figure 2b,c and Table 2).

The largest megacomplex (mc1), just entering the separation gel through the stacking gel, contained both PSI and PSII together with their antennas LHCI and LHCII (Figure 2c). This megacomplex was less abundant in *stn7* when compared with WT (Figures 4b) and S2 and Table 2]. Megacomplex 2 (mc2), present in clearly lower amounts than mc1, contained mostly PSI, but also PSII and LHCII. Mc2 was present equally between WT and *stn7*. Megacomplexes 3 and 4 (mc3 and mc4) comprised nearly exclusively PSI–LHCI, and accumulated in *stn7* in three-fold quantities as compared with WT (Figure 2b,c). Next, the megacomplex with a lower molecular mass (mc5) contained both the PSII and LHCII complexes, whereas megacomplex (mc6) consisted of PSI–LHCI. Both mc5 and mc6 were present rather equally in WT and *stn7*. Megacomplex 7 was

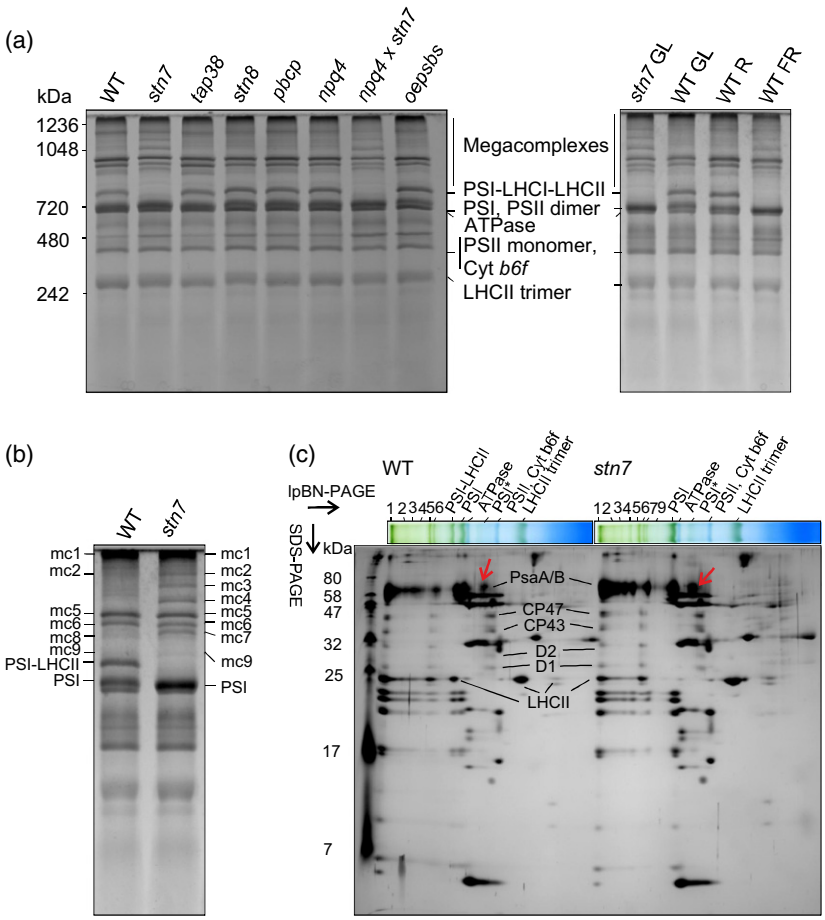

Figure 2. Composition of pigment–protein complexes in non-appressed thylakoid domains.
(a) Left panel: Thylakoid membrane megacomplex composition of WT and a set of thylakoid regulatory mutant lines. Thylakoids were isolated from growth-light-acclimated leaves, solubilized with digitonin, followed by separation of the protein complexes with lpBN-PAGE. Right panel: Comparative analyses of the digitonin-solubilized protein complexes isolated from growth-light (GL) acclimated WT and *stn7* plants as well as from WT plants exposed to red (R) or far red (FR) light for 1 h prior to thylakoids isolation. The lpBN gels were stained with Coomassie after the electrophoresis.
(b) Thylakoid membrane megacomplex (mc) composition in WT and *stn7*. Thylakoids were isolated from growth-light-acclimated leaves, solubilized with digitonin and protein complexes were separated with lpB-PAGE and stained with Coomassie blue. Protein complexes equally present in both WT and *stn7* are marked for both sides, whereas complexes present at higher quantities either in WT or in *stn7* are marked to the respective side. For nomenclature and composition of the complexes, see text.
(c) Two-dimensional lpBN/SDS-PAGE analyses of the non-appressed thylakoids of WT and *stn7*. Megacomplexes are marked with numbers to the lpBN-PAGE strips. Identification of the individual protein subunits is based on Jarvi *et al.* (2011). The red arrows indicates the PSI core complex.

present only in *stn7*, whereas the WT possessed a complex with only a slightly lower molecular mass, denoted as mc8. Both of these were composed mostly of PSI. Low abundant mc9, consisting of PSI, accumulated less in *stn7* than in WT. Finally, in line with earlier observations (Pesaresi *et al.*, 2009), *stn7* lacked the state transition-specific complex PSI–LHCI–LHCII.

Distribution of PSI among various thylakoid megacomplexes in *stn7* differs from that of WT

The composition of the megacomplexes was further verified by immunolabelling one-dimensional lpBN-PAGE gels of digitonin-solubilized thylakoids with PsaB and D1 antibodies, revealing the presence of the PSI and the PSII complexes, respectively (Figure 3). Besides containing distinct megacomplex patterns (Figure 2b,c), growth-light-acclimated WT and the *stn7* mutant also showed differences in the overall distribution of PSI and PSII in various digitonin-solubilized thylakoid membrane protein complexes, i.e. in the pigment–protein complexes located in the non-appressed thylakoid domains. The abundance of the PSI core subunit PsaB in megacomplexes 3, 4 and 7 was high in the *stn7* mutant compared with the respective complexes in the WT (Figure 3). Furthermore, even though the majority of PSI was found to be associated with megacomplexes, the *stn7* mutant had consistently more PsaA/B proteins than the WT (or *tap38*) in a complex that co-migrated with FNR, TIC62 and FTSH (Figure 1), but lacked the LHCI antenna and thus migrated faster than the PSI–LHCI complex (hereafter denoted as the PSI core and marked with a red arrow in Figure 2c). WT and *tap38* plants had a similar distribution of PsaB among protein complexes (Figure 3). As to the PSII complexes, immunoblotting of the lpBN gel with the D1 antibody revealed a similar distribution of PSII between WT, *stn7* and *tap38*; most of the D1 protein was present in PSII monomers and in megacomplexes, particularly in mc5, whereas the amount of PSII dimers was low. The Cyt b_6f complex was not detected in the megacomplexes, instead, it was found to be present as a dimer in all genotypes (Figure 3). Anti-LHCII detection on the lpBN gel revealed that mc5 and mc6 contained most of the LHCII associated with megacomplexes (Figure 3).

Short-term light acclimation modifies the composition of protein complexes in the non-appressed, but not in the appressed, thylakoid regions

The difference in the megacomplex composition between the *stn7* mutant and WT as well as that between the

Table 2 A summary of the composition, presence and light-induced dynamics of thylakoid membrane megacomplexes in the WT and the *stn7* mutant

Megacomplex	Composition	Differences in the presence between WT (100%) and *stn7* [a]	Other characteristics
mc1	PSI, PSII	More in WT (*stn7*: 79 ± 9%)	
mc2	PSI, PSII	Equally present (*stn7*: 98 ± 0.4%)	
mc3	PSI	Less in WT (*stn7*: 393 ± 47%)	In WT, accumulates under darkness, diminishes upon shift to low light
mc4	PSI	Less in WT (*stn7*: 304 ± 55%)	In WT, accumulates under darkness, diminishes upon shift to low light
mc5	PSII	Equally present (*stn7*: 111 ± 17%)	
mc6	PSI	Equally present (*stn7*: 112 ± 12%)	
mc7	PSI	Not present in WT	
mc8	PSI–LHCII	Not present in *stn7*	In WT, not present under darkness, but accumulates upon shift to light. Constitutively present in *tap38*
mc9	PSI	More in WT (*stn7*: 81 ± 7%)	Present at very low quantities

[a]The presence of the megacomplexes was quantified from light-acclimated thylakoids, and is expressed as means and standard deviations, $n = 3$–5.

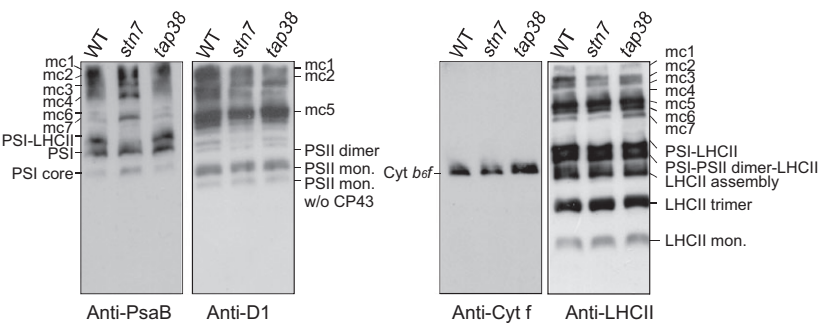

Figure 3. Immunoblot analyses of the distribution of PSI, PSII and LHCII in non-appressed thylakoid domains.
Thylakoids were isolated from growth-light-acclimated wild type (WT), *stn7* and *tap38*, solubilized with digitonin, separated with lpBN gel electrophoresis and subsequently immunolabelled with diagnostic antibodies representing PSI (anti-PsaB), PSII (anti-D1), Cyt b_6f (anti-Cyt f) and LHCII (anti-LHCII). mc, megacomplex.

treatments of WT plants with the state lights (Figure 2a) revealed a strict correlation between LHCII phosphorylation and the composition of the pigment–protein megacomplexes in non-appressed thylakoid domains. To further verify such a connection, WT, *stn7* and *tap38* plants were first acclimated to darkness for 16 h (dark samples), then shifted to low light (20 μmol photons m^{-2} sec^{-1}) for 3 h [low light (LL) 3 h samples] and finally to high light (800 μmol photons m^{-2} sec^{-1}) for an additional 3 h [high light (HL) 3 h samples], followed by gentle and rapid thylakoid isolation from fresh leaves immediately after each light treatment.

Changes in LHCII phosphorylation in the course of the light shifts were determined first. As shown in Figure 4(a), in WT plants LHCII was only slightly phosphorylated after a 16-h night (darkness) period, whereas the shift to LL induced strong phosphorylation of LHCII. Subsequent shifts of leaves to HL reduced LHCII phosphorylation. Predictably, the *stn7* mutant showed no LHCII phosphorylation under any light treatment. The *tap38* mutant LHCII, in turn, was already highly phosphorylated in the dark and this situation hardly changed during the shift to LL and then further to HL. In contrast, phosphorylation of the PSII core proteins (D1, D2 and CP43) in WT plants showed a modest decrease upon shift from darkness to LL, but a drastic increase in phosphorylation occurred as a result of the shift to HL. The *stn7* PSII core proteins were less phosphorylated compared with those of WT under darkness, whereas they were learly more phosphorylated under LL. In *tap38*, PSII core protein phosphorylation decreased upon shift from darkness to LL, and the level of phosphorylation both in darkness and low light was clearly lower compared with the WT. PSII core proteins were strongly and rather similarly phosphorylated under HL in all three genotypes. Unlike the WT that showed decreased LHCII phosphorylation upon shift to HL, *tap38* kept simultaneous high phosphorylation levels of both the PSII core and LHCII proteins under HL (Figure 4a).

An lpBN-PAGE analysis of the protein complexes in non-appressed thylakoid regions was next performed from thylakoids whose phosphorylation pattern is described above. The PSI–LHCI–LHCII complex was present only at very low amounts in dark-acclimated WT plants (Figure 4b), and in line with the low phosphorylation level of LHCII

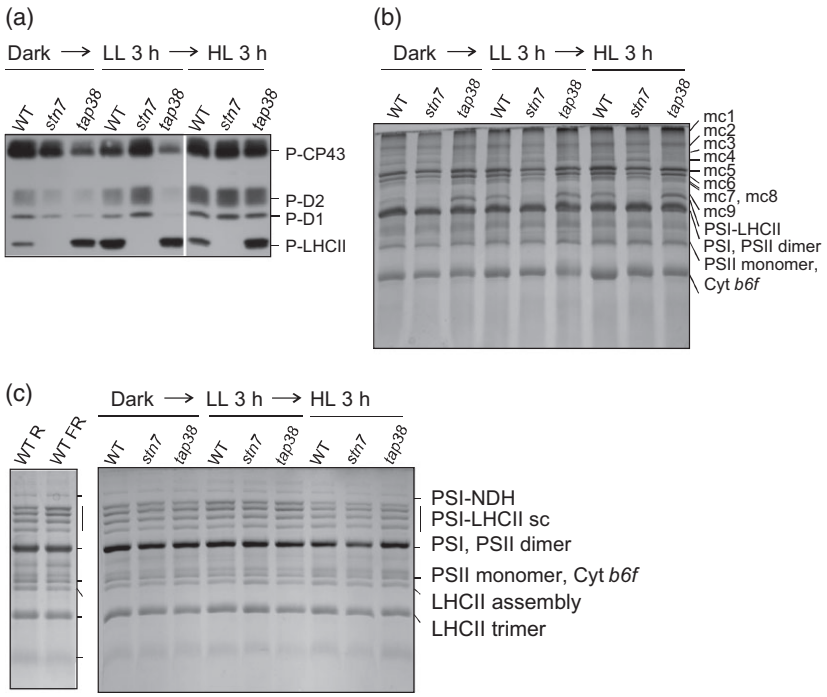

Figure 4. Dynamics of thylakoid membrane proteins and protein complexes in response to varying light conditions in WT, *stn7* and *tap38*.
Thylakoids were isolated from plants acclimated to darkness, then shifted to low light (LL) for 3 h and subsequently to high light (HL) for another 3 h.
(a) Immunoblot analyses of the PSII core (P-CP43, P-D2 and P-D1) and LHCII (P-LHCII) phosphoproteins from whole thylakoids, separated by SDS-PAGE.
(b) Composition of the protein complexes in non-appressed thylakoid domains. The thylakoids were solubilized with digitonin and separated with lpBN-PAGE. The gel was stained with Coomassie blue after electrophoresis.
(c) Composition of protein complexes in the appressed thylakoid domains. The thylakoids were solubilized with dodecyl maltoside and separated with lpBN-PAGE. The gel was stained with Coomassie blue. mc, megacomplex.

(Figure 4a). Likewise, the mc3 and mc4 complexes, which were almost missing from the growth-light-acclimated WT (Figure 2b and Table 2), were present in the dark-acclimated WT at quantities comparable with that of *stn7* (Figure 4b). Furthermore, the mc7 complex was present in the WT under darkness, whereas the mc8 complex was hardly detectable. A shift of WT plants to LL induced a pronounced increase in the content of the state transition-specific complex as well as that of mc8. mc8 was already highly abundant in *tap38* under darkness and, in general, the overall pattern of megacomplexes in *tap38* was highly similar irrespective of previous light conditions, and in line with the constant high level of its LHCII phosphorylation. Similarly, the megacomplex pattern of *stn7* also remained stable over the course of light treatments. Importantly, the pattern of digitonin-solubilized megacomplexes was highly dynamic only in WT plants, i.e. in darkness it resembled that of *stn7* but under LL it resembled that of *tap38* (Figure 4b). These modulations occurred in parallel with changes in the level of LHCII phosphorylation (Figure 4a).

As contrasting results can be found in the literature concerning the stability of the grana-located PSII–LHCII supercomplexes upon changes in light conditions (Dietzel *et al.*, 2011; Wientjes *et al.*, 2013b), we next addressed this question by investigating thylakoids from WT Arabidopsis plants that had been grown under normal white light and subsequently treated with either different qualities (PSII- or PSI-specific lights as in Dietzel *et al.*, 2011), or quantities of light, as in Wientjes *et al.* (2013b). As in both of the above-mentioned studies, isolated thylakoids were solubilized with β-dodecyl maltoside (DM) that effectively solubilizes entire thylakoids (Jarvi *et al.*, 2011), including the inner grana areas with dense arrays of PSII–LHCII supercomplexes. In addition, *stn7* and *tap38* mutants were included in the light quantity experiment to reveal whether they exhibited distinct PSII–LHCII dynamics as compared with the WT. Importantly, thylakoids were isolated gently and directly after the light treatments to avoid artificial disassembly of the supercomplexes due to freeze–thaw cycles.

WT thylakoids isolated from plants treated beforehand with either far red or red light, specifically exciting either PSI or PSII, respectively, showed minor readjustments in their PSII–LHCII composition (Figure 4c). In particular, the content of the two PSII–LHCII supercomplex oligomers (denoted as the 'B10' and 'B11' fractions in Caffarri *et al.*, 2009) accumulated under far red light treatment, while under red light all four prominent PSII–LHCII complexes (B8–B11 in Caffarri *et al.*, 2009) were present in more equal amounts. Nevertheless, the extent of these differences was far less than that reported in Dietzel *et al.* (2011). Analysis of the LHCII–PSII supercomplexes upon changing light quantities revealed a general increase in the amount of PSII–LHCII supercomplexes in all genotypes upon transfer of plants from darkness to LL, with the concomitant accumulation of the 'B10 and B11' supercomplex oligomers (Figure 4c). Subsequent shift of plants from low to HL conditions decreased the amount of PSII–LHCII supercomplexes. Importantly, and in contrast exclusively with the dynamics of the non-appressed thylakoids (Figure 4b), the *stn7* and *tap38* mutants showed similar dynamics and

stability for the PSII–LHCII supercomplexes as did the WT during light quantity shifts in the plants (Figure 4c). As the DM-solubilized thylakoid membranes are mainly composed of appressed thylakoid regions, it can be concluded that the deficiency in reversible LHCII phosphorylation does not directly affect the composition of the thylakoid protein complexes in highly appressed membranes.

Functional PSI/PSII ratios are lowered in all 'state transition' mutants

The importance of properly regulated LHCII phosphorylation for the composition of thylakoid membrane megacomplexes (Figure 4) prompted us to determine whether the overall ratio of functional photosystems was affected in *stn7* and *tap38* mutants that were incapable of LHCII (de) phosphorylation. To this end, electron paramagnetic resonance (EPR) spectroscopy was applied for quantitation of PSI and PSII. In addition to *stn7* and *tap38*, the *psal* mutant [which lacks the PsaL subunit crucial for docking phosphorylated LHCII to PSI (Lunde *et al.*, 2000) and is characterized by enhanced phosphorylation of LHCII (Leoni *et al.*, 2013) as well as the *lhcb2* mutant, deficient in the STN7 kinase client protein (Pietrzykowska *et al.*, 2014) was likewise analysed. The WT thylakoids isolated from light-acclimated plants showed a PSI/PSII ratio of 1.12 (Table 3), in line with the ratio reported earlier for WT spinach thylakoids (Danielsson *et al.*, 2004). The *psal* mutant exhibited a clearly lower PSI/PSII ratio, 0.82 and, quite unexpectedly, both the *stn7* and *tap38* mutants as well as the *lhcb2* mutant demonstrated even lower relative amounts of functional PSI, the PSI/PSII ratios being below 0.7.

DISCUSSION

Elucidation of dynamic light acclimation mechanisms of the photosynthetic machinery have primarily focused on molecular details of various short-term light acclimation mechanisms, such as 'state transitions', CET, PSII repair cycle and NPQ (Pesaresi *et al.*, 2011; Nickelsen and Rengstl, 2013; Goss and Lepetit, 2014; Pribil *et al.*, 2014). Even though the role of every single regulatory protein in controlling plant light acclimation [for instance the PsbS, PGR5, STN7, TAP38/PPH1 proteins as well as a vast number of auxiliary proteins involved in the PSII repair cycle (Jarvi *et al.*, 2015)], is crucial, the plant acclimation capacity, however, is the sum and co-operation of all different mechanisms that collectively guarantee the survival of plants in changing environmental conditions (for a review see Tikkanen and Aro, 2014). Such regulatory co-operation is reflected in the modulation of the structure and function of the photosynthetic pigment–protein complexes, allowing dynamic interactions between the pigment–protein complexes to facilitate the acclimation of the photosynthetic apparatus to changing environments. Here, the dynamics of the pigment–protein complexes in non-appressed thylakoid domains were addressed to reveal the contribution of their transient re-arrangements to short-term light acclimation.

Table 3 EPR quantification of PSI and PSII from thylakoid membranes isolated from light-acclimated plants

	$TyrD^{ox}$ (a.u.)	$P700^{+}$ (a.u.)	PSI/PSII
WT	157.7	176.5	1.12
stn7	259.7	177.4	0.68
tap38	293.7	201.9	0.69
psal	281.1	231.2	0.82

a.u., arbitrary units.
Experimental error is ±5%. The amount of PSII was determined from the integration of the dark stable TyrD radical and the amount of PSI from the integration of the ferricyanide oxidized P700 radical as in Danielsson *et al.* (2004).

Non-appressed thylakoid regions host several regulatory proteins

Making advantage of selective solubilization of the thylakoid membrane by digitonin (Jarvi *et al.*, 2011), we first specifically addressed the protein and protein complex composition of the non-appressed thylakoid membrane regions, which accommodate crucial light acclimation processes such as the PSII repair cycle and CET (Leister and Shikanai, 2013; Nickelsen and Rengstl, 2013). Digitonin, besides its location-selective solubilization properties, is capable of retaining weak protein–protein interactions to a better extent than several other widely used detergents in thylakoid research (for example DM or Triton-X) (Jarvi *et al.*, 2011), thereby potentially allowing the identification of novel protein interactions. Indeed, the NPQ-trigger protein PsbS was found to be attached in non-appressed thylakoids both to megacomplexes and to a complex of lower molecular mass. Likewise, the lumenal TLP18.3 protein was localized to the PSII monomer, instead of migrating as a free protein as was previously demonstrated with DM-solubilized thylakoids (Sirpio *et al.*, 2007), thus providing additional evidence for the function of TLP18.3 in PSII repair cycle. Similar digitonin-based thylakoid solubilization approach was taken previously to demonstrate the association of the PSII auxiliary protein LOW QUANTUM YIELD OF PHOTOSYSTEM II1 with both the PSII core monomers and low molecular mass PSII oligomers (Lu *et al.*, 2011).

Some proteins, whose localization to chloroplasts is not straightforward, were detected in non-appressed thylakoid preparations. For instance, whereas the SUBA3 database (http://suba.plantenergy.uwa.edu.au/) (Heazlewood *et al.*, 2007) predicts NAD-MALATE DEHYDROGENASE2 (PMDH2) to localize either in peroxisomes, cytoplasm or chloroplasts and FORMATE DEHYDROGENASE and CYSTEINE SYNTHASE C1 in mitochondria, those proteins were detected in non-appressed thylakoids, in accordance with

other experimental evidence indicating their presence in chloroplasts (Olson *et al.*, 2000; Peltier *et al.*, 2002; Kleffmann *et al.*, 2004; Zybailov *et al.*, 2008; Tomizioli *et al.*, 2014). It is possible that these proteins show either a dual location or, more likely, are readily detached from other cellular compartments to the thylakoid fraction during isolation.

Megacomplex composition in non-appressed thylakoids is highly dynamic

Analysis of the non-appressed thylakoid domains after exposure of plants to changing light conditions, and using several thylakoid regulation mutants (*stn7*, *tap38*, *stn8*, *pbcp*, *npq4*, *oepsbs*, *ndho*, *ndh45*, *pgr5 and oetap38)* along with the WT (Figures 2 and 4), revealed distinct dynamic regulation of the thylakoid super- and megacomplexes according to illumination cues. The mutants that harbor a megacomplex composition that differed from that of WT include *stn7*, the *stn7 npq4* double mutant and *oetap38* (Figures 2a and S1). All these mutants are devoid of LHCII protein phosphorylation (Bellafiore *et al.*, 2005; Pribil *et al.*, 2010).

Intriguingly, the megacomplex pattern of the WT non-appressed thylakoids can be manipulated to resemble that of *stn7* by exposing WT plants both to far red light or darkness, both effective in elimination of LHCII phosphorylation (Figures 2a and 4a,b). Conversely, exposure of WT plants to LL resulted in a megacomplex pattern of non-appressed thylakoid domains that was similar to that of the *tap38* mutant, which exhibits maximally phosphorylated LHCII (Figure 4a,b). Taken together, changes in light conditions that drastically modulate LHCII protein phosphorylation also have a prominent effect on the composition of the pigment–protein complexes in the non-appressed thylakoid domains (Figures 2a and 4b). In contrast, the protein complexes in appressed grana thylakoids, i.e. those observed after thylakoid solubilization with DM, do not respond to changes in light conditions or differ between mutants that have a different LHCII protein phosphorylation status (Figure 4c).

Interaction between PSI and LHCII determines stable megacomplex formation and composition

Distinct differences in the *stn7* (mega)complex pattern in non-appressed thylakoids from those of WT and *tap38* (Figures 2–4 and Table 2) include the following: (i) lower amount of the highest molecular mass megacomplex (mc1), composed of both PSI and PSII; (ii) higher amounts of mc3, mc4 and mc7, all composed of PSI; (iii) absence of mc8 and the 'state transition-specific protein complex'; and (iv) higher quantities of the PSI core complex, which contains the PSI core subunits but lacks the LHCI antenna proteins (Figure 1).

There is complete absence of the mc8 megacomplex in *stn7*, which is present in *tap38* under all light conditions and in WT accumulates together with increasing LHCII phosphorylation. This absence provides evidence that, besides mc1 and the previously characterized 'state transition-specific complex' (Pesaresi *et al.*, 2009), there are also other, less abundant, megacomplex(es) in the non-appressed thylakoid domains that contain LHCII attached to PSI. In addition, the higher amounts of the PSI core complex in *stn7* may indicate either accelerated biogenesis or degradation of the PSI–LHCI complex as compared with WT.

The most fundamental difference in non-appressed thylakoids in *stn7* compared with WT is the lowered amount of mc1, the megacomplex that has the highest molecular mass and is comprised of both PSI and PSII together with their LHC antennas (Figures 2 and S2). It was recently demonstrated that the two photosystems are indeed energetically connected in non-appressed thylakoids (Yokono *et al.*, 2015), and that this connection is detectable in mc1. A functional connection between PSII and PSI is likely needed for transient balancing of the excitation energy distribution between the photosystems. For instance, energy quenching by PSI might be essential for the protection of PSII under conditions in which PSII centres are closed (Yokono *et al.*, 2015). The capability of PSII and LHCII to form highly ordered super- and megacomplexes that further form dense semicrystalline arrays in grana stacks (Dekker and Boekema, 2005; Caffarri *et al.*, 2009; Pagliano *et al.*, 2014) indicates that the connection between PSII and LHCII is strong. Thus, the integrity and firmness of the PSII–LHCII-PSI system primarily depend on the strength of the bonds between PSI and LHCII. Based on the fact that *stn7* lacks not only the 'state transition-specific complex' (PSI–LHCII) (Pesaresi *et al.*, 2009) but also mc8 (Figure 2b), it is conceivable that the integrity of the LHCII–PSI interaction is, in general, essential for megacomplex formation, the highest stability being reached by LHCII phosphorylation (Table 2). The absence of such a strong interaction in *stn7* results in a lowered amount of mc1, i.e. the PSII–LHCII–PSI, in line with impaired excitation energy distribution between the two photosystems in *stn7* (Grieco *et al.*, 2012).

Opposite to the mc1 megacomplex, *stn7* (Figures 2 and 4) and *oetap38* (Figure S1) had high amounts of the mc3 and mc4 megacomplexes, which in WT were present only under far red light (Figure 2a) and in darkness (Figure 4b). Accumulation of mc3 and mc4 thus coincides with complete lack or only a low level of LHCII phosphorylation and likely represent PSI complexes detached from the loosely cohesive PSII–LHCII–PSI megacomplex (mc1) in the absence of LHCII protein phosphorylation. Based on estimated molecular masses and on Heinemeyer *et al.* (2004), the mc3 and mc4 megacomplexes most likely represent

trimeric and dimeric forms of PSI. Nevertheless, it is of utmost importance to note that the presence of the STN7 kinase and LHCII phosphorylation as such is not sufficient for building a firm PSII–LHCII–PSI connection, i.e. the mc1 megacomplex. Indeed, previous reports on megacomplex patterns in the *lhcb2* mutant that lacks the state transition trigger protein Lhcb2 (Pietrzykowska *et al.*, 2014) and in the *psal* mutant (Leoni *et al.*, 2013) that phosphorylates LHCII but lacks the docking protein PsaL, demonstrate not only the lack of the state transition-specific complex but also a deficiency of mc1 and increased amounts of mc3 and mc4 (Leoni *et al.*, 2013; Pietrzykowska *et al.*, 2014). It is thus highly conceivable that the defective connection between PSI and LHCII, either due to the lack of LHCII protein phosphorylation or to the absence of a LHCII docking site in PSI, prevents stable PSI–PSII megacomplex (mc1) formation by provoking partial detachment of the PSI complexes, which can be visualized as mc3 and mc4.

Functional PSI:PSII ratio was lowered in all 'state transition' mutants

Dynamics in the stoichiometry of photosystems and their antennas provide functional flexibility upon various environmental and developmental conditions (reviewed in Schottler and Toth, 2014). In order to reveal whether disturbed regulation of LHCII (de)phosphorylation and megacomplex dynamics in non-appressed regions instigates changes in relative amounts of functional PSII and PSI, the PS amounts were quantified with EPR spectroscopy (Table 3). The amounts of PSI did not differ between the mutants and the WT, whilst all mutants showed higher amounts of PSII as compared with the WT. Thus, the relative ratio of functional PSI to PSII was lowered in all mutants investigated, highlighting the importance of properly regulated LHCII phosphorylation for the sustenance of a normal PSI:PSII ratio. It is highly likely that the defective excitation energy transfer along the thylakoid membrane, due to the lack of LHCII (de)phosphorylation, creates a redox unbalance which causes alterations in the ratio of functional PSI and PSII (Grieco *et al.*, 2012). Although PSII has traditionally been regarded as a most vulnerable photosystem, low-temperature-induced PSI photoinhibition has been known for decades (Havaux and Devaud, 1994; Sonoike *et al.*, 1995; Kudoh and Sonoike, 2002) and more recent reports have emphasized that actually, under certain conditions, PSI does suffer more light-induced damage than PSII (Suorsa *et al.*, 2012; Kono *et al.*, 2014).

Taken together, a model on regulation of the interaction of thylakoid protein complexes upon light acclimation, primarily occurring in the non-appressed thylakoid domains, is proposed in Figure 5. Dynamic light-induced interactions are shown to take place between pigment–protein complexes in the non-appressed thylakoid domains. It is suggested that PSII and PSI are connected at the interphases between the grana stacks and stroma membranes, and can be visualized as the PSII–LHCII–PSI megacomplex mc1. The integrity of the most fragile part of this megacomplex, i.e. the association between PSI and LHCII, is controlled both by the phosphorylation of LHCII and by the LHCII docking proteins in PSI. Light-dependent modifications in LHCII phosphorylation strengthen/loosen the PSII–LHCII–PSI connection and thereby control the maintenance of balanced energy distribution between the two photosystems.

EXPERIMENTAL PROCEDURES

Plant material and growth conditions

Arabidopsis thaliana ecotype Columbia WT as well as *stn7* (Bellafiore *et al.*, 2005), *tap38* (Pribil *et al.*, 2010; Shapiguzov *et al.*, 2010), *stn8* (Bonardi *et al.*, 2005; Vainonen *et al.*, 2005), *pbcp* (Samol *et al.*, 2012), *npq4* (Li *et al.*, 2000), *npq4 stn7* (Frenkel *et al.*, 2007), *oepsbs* (Li *et al.*, 2002), *ndho* (Rumeau *et al.*, 2005), *ndh45* (Sirpio *et al.*, 2009), *pgr5* (Munekage *et al.*, 2002) and *oetap38* (Bellafiore *et al.*, 2005) were grown in a mixture of soil and vermiculite (1:1) under a photon flux density of 120 μmol of photons·m^{-2} sec^{-1} in an 8 h light/16 h dark regime at 23°C. OSRAM PowerStar HQIT 400/D metal halide lamps were used as a light source. Mature rosette leaves from 5- to 6-week-old plants were used for the experiments. For specific experiments, the plants were treated with darkness, LL (20 μmol photons m^{-2} sec^{-1}) or HL (800 μmol photons m^{-2} sec^{-1}). The treatments with PSI- and PSII-specific lights were given as described in Tikkanen *et al.* (2010).

Thylakoid isolation and solubilization

Thylakoids were isolated from fresh leaves according to Jarvi *et al.* (2011) with 10 mM NaF included in all buffers. The chlorophyll content was measured according to (Porra *et al.*, 1989). Thylakoids were resuspended into ice-cold 25BTH20G buffer [25 mM BisTris/HCl (pH 7.0), 20% (w/v) glycerol, 0.25 mg ml^{-1} Pefabloc], and an equal volume of detergent solution (diluted in 25BTH20G buffer) to a final concentration of 1% (w/v) digitonin (Calbiochem, www.calbiochem.com) or DM (Sigma-Aldrich, https://www.sigmaaldrich.com) was added. Importantly, digitonin was purified according to manufacturer's instructions prior to use. Thylakoids were solubilized in room temperature with continuous gentle mixing for 10 min when using digitonin, or on ice for 5 min when using DM. The insoluble material was pelleted by centrifugation at 18 000 ***g*** at 4°C for 25 min and the supernatant was supplemented with a 1/10 volume of loading buffer as in Jarvi *et al.* (2011) prior to electrophoresis. For one-dimensional SDS-PAGE, the thylakoids were solubilized according to Laemmli (1970).

Gel electrophoresis, immunoblotting and mass spectrometry

The solubilized thylakoid membrane protein complexes were separated with lpBN-PAGE as described in Jarvi *et al.* (2011). After the run, the lpBN gels were scanned, and either stained with Coomassie blue (40% MeOH, 10% acetic acid, 0.1% CBB-R9-50) for better visualization of the protein complexes, or electroblotted to a polyvinylidene difluoride (PVDF) membrane (Millipore, https://www.emdmillipore.com) or subjected to two-dimensional (2D) SDS-PAGE for separation of the distinct subunits of the protein complexes (Jarvi *et al.*, 2011). The bands from the Coomassie-stained gels were quantified with Gene Tools software from Perk-

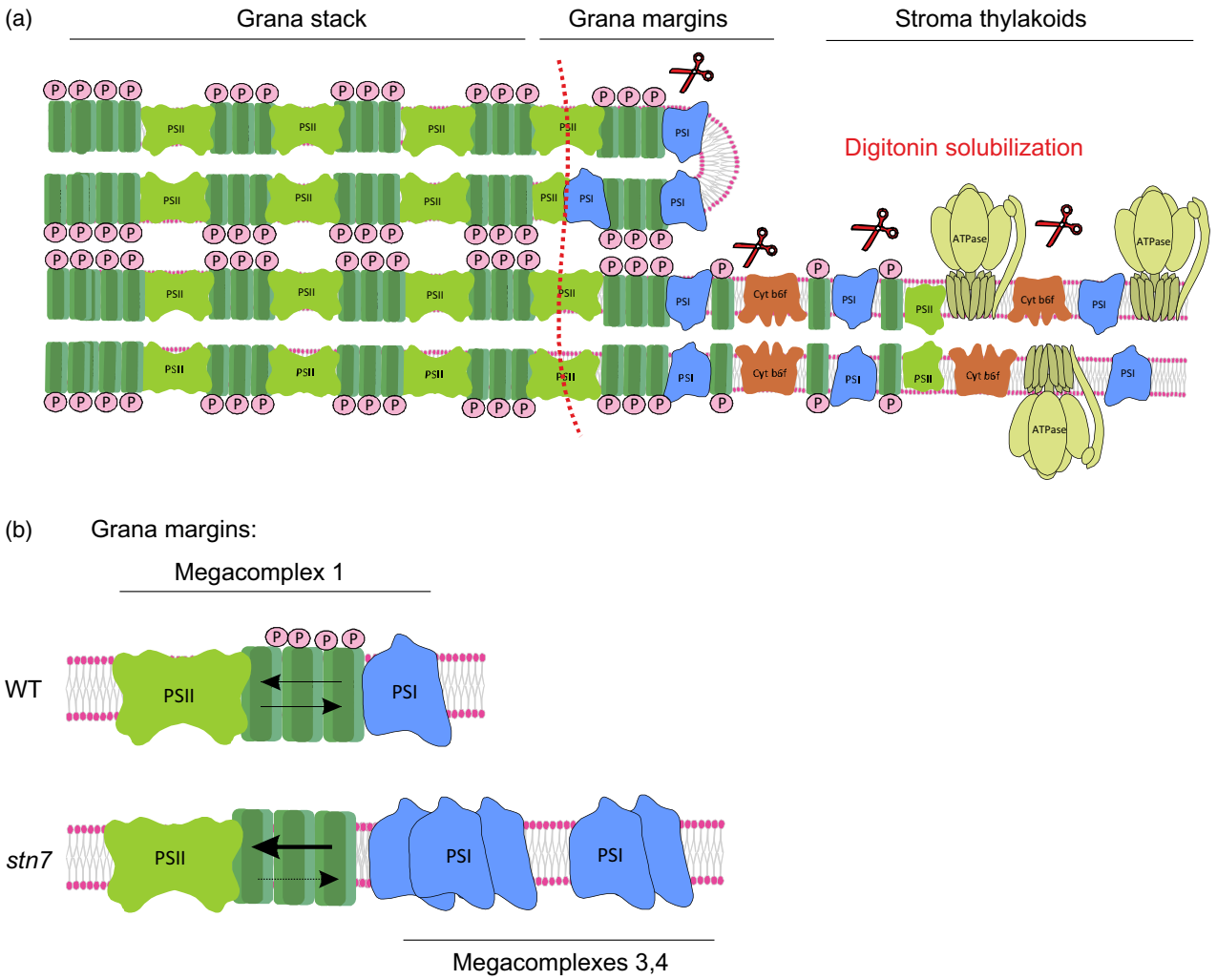

Figure 5. Schematic model for dynamics of pigment–protein complexes upon light acclimation.
(a) Thylakoid membrane protein complexes exhibit lateral heterogeneity in their distribution: PSII is mostly located in grana stacks, whereas PSI, Cyt b_6f and the ATP synthase are mostly found in the stroma-exposed thylakoid membranes. Yet, the interphase of appressed and non-appressed membrane contains both PSI and PSII and is the most dynamic region of the thylakoid membrane in response to changing light conditions. Digitonin preferentially solubilizes the non-appressed thylakoids (depicted as scissors and dashed line).
(b) Both photosystems are connected in the grana margins in WT (megacomplex 1). In *stn7*, the lack of LHCII phosphorylation loosens the connection between the LHCII and PSI, which results in scarcity of the megacomplex 1 (mc1). Instead, the PSI complexes detached from megacomplex 1 are detected as megacomplexes 3 and 4.

inElmer (http://www.perkinelmer.com). The proteins from the 2D gels were visualized by silver staining. For protein identification, in-gel trypsin digestion and subsequent analysis of the eluted peptides by mass spectrometry was performed as in Li *et al.* (2014), except that some spots were identified with a LTQ Orbitrap Velos Pro (ThermoScientific, www.thermoscientific.com).

For one-dimensional SDS-PAGE, gels with 15% (w/v) polyacrylamide and 6 M urea were run overnight with constant current of 8–10 mA. The gels were loaded on an equal chlorophyll basis. After electrophoresis the proteins were electroblotted to a PVDF membrane. The phosphothreonine antibody was purchased from New England Biolabs (https://www.neb.com), and the antibodies against PsaB and Cyt f from Agrisera (www.agrisera.com, catalogue numbers AS10695 and A506119, respectively) . Horseradish peroxidase-linked secondary antibody and enhanced chemiluminescence reagents (Amersham, GE Healthcare, www.gehealthcare.com) were used for detection.

Quantification of the PSs

Room temperature continuous wave (CW) EPR was performed essentially as described in Danielsson *et al.* (2004). Measurements were performed in a flat cell at room temperature with a Bruker ELEXSYS E500 spectrometer equipped with a SuperX bridge and SHCE4122 resonator (Bruker BioSpin GmbH, www.bruker.com). All measurements were done at the same Chl concentration of 2 mg ml^{-1}.

ACKNOWLEDGEMENTS

Our research was financially supported by the Academy of Finland (project numbers 271832 and 273870), the Swedish Research Council, the Swedish Energy Agency, the Knut and Alice Wallenberg Foundation and the Initial Training Network (ITN) CALIPSO (GA ITN 2013-607-607). We thank Dario Leister for providing the

tap38 and *oetap38* mutants, Jean-David Rochaix for the *pbcp* and *stn7 npq4* mutants, Krishna Niyogi for the *npq4* mutant, Toshiharu Shikanai for the *pgr5* mutant, Dominique Rumeau for the *ndho* mutant and Stefan Jansson for the *oepsbs* mutant. The Proteomic unit of the Turku Centre for Biotechnology is thanked for assistance with mass spectrometry. Virpi Paakkarinen and Mika Keränen are acknowledged for their excellent technical assistance.

CONFLICT OF INTERESTS

The authors have no conflicts of interest.

SUPPORTING INFORMATION

Additional Supporting Information may be found in the online version of this article.

Figure S1. Megacomplexes composition in non-appressed thylakoid domains of cyclic electron transfer and 'state transition' mutants.

Figure S2. Non-stained lpBN from digitonin-solubilized thylakoid membrane protein complexes of WT and stn7.

REFERENCES

Albertsson, P. (2001) A quantitative model of the domain structure of the photosynthetic membrane. *Trends Plant Sci.* **6**(8), 349–354.

Anderson, J.M., Horton, P., Kim, E.H. and Chow, W.S. (2012) Towards elucidation of dynamic structural changes of plant thylakoid architecture. *Philos. Trans. R. Soc. Lond. B Biol. Sci.* **367**(1608), 3515–3524.

Armbruster, U., Labs, M., Pribil, M. *et al.* (2013) Arabidopsis CURVATURE THYLAKOID1 proteins modify thylakoid architecture by inducing membrane curvature. *Plant Cell*, **25**(7), 2661–2678.

Bellafiore, S., Barneche, F., Peltier, G. and Rochaix, J.D. (2005) State transitions and light adaptation require chloroplast thylakoid protein kinase STN7. *Nature*, **433**(7028), 892–895.

Benz, J.P., Stengel, A., Lintala, M. *et al.* (2009) Arabidopsis Tic62 and ferredoxin-NADP(H) oxidoreductase form light-regulated complexes that are integrated into the chloroplast redox poise. *Plant Cell*, **21**(12), 3965–3983.

Bonardi, V., Pesaresi, P., Becker, T., Schleiff, E., Wagner, R., Pfannschmidt, T., Jahns, P. and Leister, D. (2005) Photosystem II core phosphorylation and photosynthetic acclimation require two different protein kinases. *Nature*, **437**(7062), 1179–1182.

Brautigam, K., Dietzel, L., Kleine, T. *et al.* (2009) Dynamic plastid redox signals integrate gene expression and metabolism to induce distinct metabolic states in photosynthetic acclimation in Arabidopsis. *Plant Cell*, **21**(9), 2715–2732.

Caffarri, S., Kouril, R., Kereiche, S., Boekema, E.J. and Croce, R. (2009) Functional architecture of higher plant photosystem II supercomplexes. *EMBO J.* **28**(19), 3052–3063.

Danielsson, R. and Albertsson, P.A. (2009) Fragmentation and separation analysis of the photosynthetic membrane from spinach. *Biochim. Biophys. Acta*, **1787**(1), 25–36.

Danielsson, R., Albertsson, P.A., Mamedov, F. and Styring, S. (2004) Quantification of photosystem I and II in different parts of the thylakoid membrane from spinach. *Biochim. Biophys. Acta*, **1608**(1), 53–61.

Dekker, J. and Boekema, E. (2005) Supramolecular organization of thylakoid membrane proteins in green plants. *Biochim. Biophys. Acta*, **1706**(1–2), 12–39.

Dietzel, L., Brautigam, K., Steiner, S., Schuffler, K., Lepetit, B., Grimm, B., Schottler, M.A. and Pfannschmidt, T. (2011) Photosystem II supercomplex remodeling serves as an entry mechanism for state transitions in Arabidopsis. *Plant Cell*, **23**(8), 2965–2977.

Frenkel, M., Bellafiore, S., Rochaix, J. and Jansson, S. (2007) Hierarchy amongst photosynthetic acclimation responses for plant fitness. *Physiol. Plant.* **129**(2), 455–459.

Galka, P., Santabarbara, S., Khuong, T.T., Degand, H., Morsomme, P., Jennings, R.C., Boekema, E.J. and Caffarri, S. (2012) Functional analyses of the plant photosystem I-light-harvesting complex II supercomplex reveal that light-harvesting complex II loosely bound to photosystem II is a very efficient antenna for photosystem I in state II. *Plant Cell*, **24**(7), 2963–2978.

Gao, H., Sage, T.L. and Osteryoung, K.W. (2006) FZL, an FZO-like protein in plants, is a determinant of thylakoid and chloroplast morphology. *Proc. Natl. Acad. Sci. USA*, **103**(17), 6759–6764.

Goss, R. and Lepetit, B. (2014) Biodiversity of NPQ. *J. Plant Physiol.* **172**, 13–32.

Grieco, M., Tikkanen, M., Paakkarinen, V., Kangasjarvi, S. and Aro, E.M. (2012) Steady-state phosphorylation of light-harvesting complex II proteins preserves photosystem I under fluctuating white light. *Plant Physiol.* **160**(4), 1896–1910.

Grieco, M., Suorsa, M., Jajoo, A., Tikkanen, M. and Aro, E.M. (2015) Light-harvesting II antenna trimers connect energetically the entire photosynthetic machinery – including both photosystems II and I. *Biochim. Biophys. Acta*, **1847**(6–7), 607–619.

Havaux, M. and Devaud, A. (1994) Photoinhibition of photosynthesis in chilled potato leaves is not correlated with a loss of photosystem-ii activity – preferential inactivation of photosystem-i. *Photosynth. Res.* **40**(1), 75–92.

Heazlewood, J.L., Verboom, R.E., Tonti-Filippini, J., Small, I. and Millar, A.H. (2007) SUBA: the Arabidopsis subcellular database. *Nucleic Acids Res.* **35**(Database issue), D213–D218.

Heinemeyer, J., Eubel, H., Wehmhoner, D., Jansch, L. and Braun, H.P. (2004) Proteomic approach to characterize the supramolecular organization of photosystems in higher plants. *Phytochemistry*, **65**(12), 1683–1692.

Herbstova, M., Tietz, S., Kinzel, C., Turkina, M.V. and Kirchhoff, H. (2012) Architectural switch in plant photosynthetic membranes induced by light stress. *Proc. Natl. Acad. Sci. USA*, **109**(49), 20130–20135.

Iwai, M., Yokono, M. and Nakano, A. (2014) Visualizing structural dynamics of thylakoid membranes. *Sci. Rep.* **4**, 3768.

Jarvi, S., Suorsa, M., Paakkarinen, V. and Aro, E.M. (2011) Optimized native gel systems for separation of thylakoid protein complexes: novel super- and mega-complexes. *Biochem. J.* **439**(2), 207–214.

Jarvi, S., Suorsa, M. and Aro, E.M. (2015) Photosystem II repair in plant chloroplasts – regulation, assisting proteins and shared components with photosystem II biogenesis. *Biochim. Biophys. Acta*, **1847**(9), 900–909.

Kettunen, R., Tyystjärvi, E. and Aro, E.M. (1995) Do grana margins form a functional domain during photosystem II repair cycle? In *Photosynthesis: From Light to Biosphere*, Vol. 4 (Mathis, P., ed). Dordrecht, the Netherlands: Kluwer Academic Publishers, pp. 331.

Kirchhoff, H. (2013) Architectural switches in plant thylakoid membranes. *Photosynth. Res.* **116**(2–3), 481–487.

Kirchhoff, H., Mukherjee, U. and Galla, H.J. (2002) Molecular architecture of the thylakoid membrane: lipid diffusion space for plastoquinone. *Biochemistry*, **41**(15), 4872–4882.

Kirchhoff, H., Tremmel, I., Haase, W. and Kubitscheck, U. (2004) Supramolecular photosystem II organization in grana thylakoid membranes: evidence for a structured arrangement. *Biochemistry*, **43**(28), 9204–9213.

Kleffmann, T., Russenberger, D., von Zychlinski, A., Christopher, W., Sjolander, K., Gruissem, W. and Baginsky, S. (2004) The *Arabidopsis thaliana* chloroplast proteome reveals pathway abundance and novel protein functions. *Curr. Biol.* **14**(5), 354–362.

Kono, M., Noguchi, K. and Terashima, I. (2014) Roles of the cyclic electron flow around PSI (CEF-PSI) and O(2)-dependent alternative pathways in regulation of the photosynthetic electron flow in short-term fluctuating light in *Arabidopsis thaliana*. *Plant Cell Physiol.* **55**(5), 990–1004.

Kouril, R., Wientjes, E., Bultema, J.B., Croce, R. and Boekema, E.J. (2013) High-light vs. low-light: effect of light acclimation on photosystem II composition and organization in *Arabidopsis thaliana*. *Biochim. Biophys. Acta*, **1827**(3), 411–419.

Kubigsteltig, I., Laudert, D. and Weiler, E.W. (1999) Structure and regulation of the *Arabidopsis thaliana* allene oxide synthase gene. *Planta*, **208**(4), 463–471.

Kudoh, H. and Sonoike, K. (2002) Irreversible damage to photosystem I by chilling in the light: cause of the degradation of chlorophyll after returning to normal growth temperature. *Planta*, **215**(4), 541–548.

Laemmli, U.K. (1970) Cleavage of structural proteins during the assembly of the head of bacteriophage T4. *Nature*, **227**(5259), 680–685.

Laudert, D., Pfannschmidt, U., Lottspeich, F., Hollander-Czytko, H. and Weiler, E.W. (1996) Cloning, molecular and functional characterization of

Arabidopsis thaliana allene oxide synthase (CYP 74), the first enzyme of the octadecanoid pathway to jasmonates. *Plant Mol. Biol.* **31**(2), 323–335.

Leister, D. and Shikanai, T. (2013) Complexities and protein complexes in the antimycin A-sensitive pathway of cyclic electron flow in plants. *Front. Plant Sci.* **4**, 161.

Leoni, C., Pietrzykowska, M., Kiss, A.Z., Suorsa, M., Ceci, L.R., Aro, E.M. and Jansson, S. (2013) Very rapid phosphorylation kinetics suggest a unique role for Lhcb2 during state transitions in Arabidopsis. *Plant J.* **76** (2), 236–246.

Li, X.P., Bjorkman, O., Shih, C., Grossman, A.R., Rosenquist, M., Jansson, S. and Niyogi, K.K. (2000) A pigment-binding protein essential for regulation of photosynthetic light harvesting. *Nature*, **403**(6768), 391–395.

Li, X.P., Muller-Moule, P., Gilmore, A.M. and Niyogi, K.K. (2002) PsbS-dependent enhancement of feedback de-excitation protects photosystem II from photoinhibition. *Proc. Natl Acad. Sci. USA*, **99**(23), 15222–15227.

Li, S., Mhamdi, A., Trotta, A., Kangasjarvi, S. and Noctor, G. (2014) The protein phosphatase subunit PP2A-B'gamma is required to suppress day length-dependent pathogenesis responses triggered by intracellular oxidative stress. *New Phytol.* **202**(1), 145–160.

Lintala, M., Schuck, N., Thormahlen, I., Jungfer, A., Weber, K.L., Weber, A.P., Geigenberger, P., Soll, J., Bolter, B. and Mulo, P. (2014) Arabidopsis tic62 trol mutant lacking thylakoid-bound ferredoxin-NADP+ oxidoreductase shows distinct metabolic phenotype. *Mol. Plant* **7**(1), 45–57.

Lu, Y., Hall, D.A. and Last, R.L. (2011) A small zinc finger thylakoid protein plays a role in maintenance of photosystem II in *Arabidopsis thaliana*. *Plant Cell*, **23**(5), 1861–1875.

Lunde, C., Jensen, P.E., Haldrup, A., Knoetzel, J. and Scheller, H.V. (2000) The PSI-H subunit of photosystem I is essential for state transitions in plant photosynthesis. *Nature*, **408**(6812), 613–615.

Munekage, Y., Hojo, M., Meurer, J., Endo, T., Tasaka, M. and Shikanai, T. (2002) PGR5 is involved in cyclic electron flow around photosystem I and is essential for photoprotection in Arabidopsis. *Cell*, **110**(3), 361–371.

Nickelsen, J. and Rengstl, B. (2013) Photosystem II assembly: from cyanobacteria to plants. *Annu. Rev. Plant Biol.* **64**, 609–635.

Olson, B.J., Skavdahl, M., Ramberg, H., Osterman, J.C. and Markwell, J. (2000) Formate dehydrogenase in *Arabidopsis thaliana*: characterization and possible targeting to the chloroplast. *Plant Sci.* **159**(2), 205–212.

Pagliano, C., Nield, J., Marsano, F., Pape, T., Barera, S., Saracco, G. and Barber, J. (2014) Proteomic characterization and three-dimensional electron microscopy study of PSII–LHCII supercomplexes from higher plants. *Biochim. Biophys. Acta*, **1837**(9), 1454–1462.

Peltier, J.B., Emanuelsson, O., Kalume, D.E. *et al.* (2002) Central functions of the lumenal and peripheral thylakoid proteome of Arabidopsis determined by experimentation and genome-wide prediction. *Plant Cell*, **14** (1), 211–236.

Peng, L., Shimizu, H. and Shikanai, T. (2008) The chloroplast NAD(P)H dehydrogenase complex interacts with photosystem I in Arabidopsis. *J. Biol. Chem.* **283**(50), 34873–34879.

Pesaresi, P., Hertle, A., Pribil, M. *et al.* (2009) Arabidopsis STN7 kinase provides a link between short- and long-term photosynthetic acclimation. *Plant Cell*, **21**(8), 2402–2423.

Pesaresi, P., Pribil, M., Wunder, T. and Leister, D. (2011) Dynamics of reversible protein phosphorylation in thylakoids of flowering plants: the roles of STN7, STN8 and TAP38. *Biochim. Biophys. Acta*, **1807**(8), 887–896.

Pietrzykowska, M., Suorsa, M., Semchonok, D.A., Tikkanen, M., Boekema, E.J., Aro, E.M. and Jansson, S. (2014) The light-harvesting chlorophyll *a*/*b* binding proteins Lhcb1 and Lhcb2 play complementary roles during state transitions in Arabidopsis. *Plant Cell*, **26**(9), 3646–3660.

Porra, R.J., Thompson, W.A. and Kriedemann, P.E. (1989) Determination of accurate extinction coefficients and simultaneous-equations for assaying chlorophyll-a and chlorophyll-B extracted with four different solvents – verification of the concentration of chlorophyll standards by atomic-absorption spectroscopy. *Biochim. Biophys. Acta*, **975**(3), 384–394.

Pribil, M., Pesaresi, P., Hertle, A., Barbato, R. and Leister, D. (2010) Role of plastid protein phosphatase TAP38 in LHCII dephosphorylation and thylakoid electron flow. *PLoS Biol.* **8**(1), e1000288.

Pribil, M., Labs, M. and Leister, D. (2014) Structure and dynamics of thylakoids in land plants. *J. Exp. Bot.* **65**(8), 1955–1972.

Rumeau, D., Becuwe-Linka, N., Beyly, A., Louwagie, M., Garin, J. and Peltier, G. (2005) New subunits NDH-M, -N, and -O, encoded by nuclear genes, are essential for plastid ndh complex functioning in higher plants. *Plant Cell*, **17**(1), 219–232.

Samol, I., Shapiguzov, A., Ingelsson, B., Fucile, G., Crevecoeur, M., Vener, A.V., Rochaix, J.D. and Goldschmidt-Clermont, M. (2012) Identification of a photosystem II phosphatase involved in light acclimation in Arabidopsis. *Plant Cell*, **24**(6), 2596–2609.

Schottler, M.A. and Toth, S.Z. (2014) Photosynthetic complex stoichiometry dynamics in higher plants: environmental acclimation and photosynthetic flux control. *Front. Plant Sci.* **5**, 188.

Shapiguzov, A., Ingelsson, B., Samol, I., Andres, C., Kessler, F., Rochaix, J.D., Vener, A.V. and Goldschmidt-Clermont, M. (2010) The PPH1 phosphatase is specifically involved in LHCII dephosphorylation and state transitions in Arabidopsis. *Proc. Natl Acad. Sci. USA*, **107**(10), 4782–4787.

Sirpio, S., Allahverdiyeva, Y., Suorsa, M., Paakkarinen, V., Vainonen, J., Battchikova, N. and Aro, E.M. (2007) TLP18.3, a novel thylakoid lumen protein regulating photosystem II repair cycle. *Biochem. J.* **406**(3), 415–425.

Sirpio, S., Allahverdiyeva, Y., Holmstrom, M., Khrouchtchova, A., Haldrup, A., Battchikova, N. and Aro, E.M. (2009) Novel nuclear-encoded subunits of the chloroplast NAD(P)H dehydrogenase complex. *J. Biol. Chem.* **284** (2), 905–912.

Sonoike, K., Terashima, I., Iwaki, M. and Itoh, S. (1995) Destruction of photosystem I iron-sulfur centers in leaves of cucumis sativus L. by weak illumination at chilling temperatures. *FEBS Lett.* **362**(2), 235–238.

Strecker, V., Wumaier, Z., Wittig, I. and Schagger, H. (2010) Large pore gels to separate mega protein complexes larger than 10 MDa by blue native electrophoresis: isolation of putative respiratory strings or patches. *Proteomics*, **10**(18), 3379–3387.

Suorsa, M., Järvi, S., Grieco, M. *et al.* (2012) PROTONGRADIENTREGULATION5 is essential for proper acclimation of Arabidopsis Photosystem I to naturally and artificially fluctuating light conditions. *Plant Cell*, **24**, 2934–2948.

Suorsa, M., Rantala, M., Danielsson, R., Jarvi, S., Paakkarinen, V., Schroder, W.P., Styring, S., Mamedov, F. and Aro, E.M. (2014) Dark-adapted spinach thylakoid protein heterogeneity offers insights into the photosystem II repair cycle. *Biochim. Biophys. Acta*, **1837**(9), 1463–1471.

Tietz, S., Puthiyaveetil, S., Enlow, H.M. *et al.* (2015) Functional implications of photosystem II crystal formation in photosynthetic membranes. *J. Biol. Chem.* **290**(22), 14091–14106.

Tikkanen, M. and Aro, E.M. (2014) Integrative regulatory network of plant thylakoid energy transduction. *Trends Plant Sci.* **19**(1), 10–17.

Tikkanen, M., Piippo, M., Suorsa, M., Sirpio, S., Mulo, P., Vainonen, J., Vener, A.V., Allahverdiyeva, Y. and Aro, E.M. (2006) State transitions revisited-a buffering system for dynamic low light acclimation of Arabidopsis. *Plant Mol. Biol.* **62**(4–5), 779–793.

Tikkanen, M., Grieco, M., Kangasjarvi, S. and Aro, E.M. (2010) Thylakoid protein phosphorylation in higher plant chloroplasts optimizes electron transfer under fluctuating light. *Plant Physiol.* **152**(2), 723–735.

Tomizioli, M., Lazar, C., Brugiere, S. *et al.* (2014) Deciphering thylakoid subcompartments using a mass spectrometry-based approach. *Mol. Cell Proteomics*, **13**(8), 2147–2167.

Vainonen, J.P., Hansson, M. and Vener, A.V. (2005) STN8 protein kinase in *Arabidopsis thaliana* is specific in phosphorylation of photosystem II core proteins. *J. Biol. Chem.* **280**(39), 33679–33686.

Vainonen, J.P., Sakuragi, Y., Stael, S. *et al.* (2008) Light regulation of CaS, a novel phosphoprotein in the thylakoid membrane of *Arabidopsis thaliana*. *FEBS J.* **275**(8), 1767–1777.

Wagner, R., Aigner, H. and Funk, C. (2012) FtsH proteases located in the plant chloroplast. *Physiol. Plant.* **145**(1), 203–214.

Wientjes, E., van Amerongen, H. and Croce, R. (2013a) LHCII is an antenna of both photosystems after long-term acclimation. *Biochim. Biophys. Acta*, **1827**(3), 420–426.

Wientjes, E., Drop, B., Kouril, R., Boekema, E.J. and Croce, R. (2013b) During state 1 to state 2 transition in *Arabidopsis thaliana*, the photosystem II supercomplex gets phosphorylated but does not disassemble. *J. Biol. Chem.* **288**(46), 32821–32826.

Yokono, M., Takabayashi, A., Akimoto, S. and Tanaka, A. (2015) A megacomplex composed of both photosystem reaction centres in higher plants. *Nat. Commun.* **6**, 6675.

Zybailov, B., Rutschow, H., Friso, G., Rudella, A., Emanuelsson, O., Sun, Q. and van Wijk, K.J. (2008) Sorting signals, N-terminal modifications and abundance of the chloroplast proteome. *PLoS ONE*, **3**(4), e1994.